Nuclear Instruments and Methods in Physics Research A 659 (2011) 154–160

Contents lists available at ScienceDirect

Nuclear Instruments and Methods in Physics Research A

journal homepage: www.elsevier.com/locate/nima

The mass production and quality control of RPCs for the Daya Bay experiment

Liehua Ma [a,b,1], Logan Lebanowski [c], Jin Chen [a], Mengyun Guan [a], Robert Hackenburg [d], Kwong Lau [c], Shih-Kai Lin [c], Changguo Lu [e], Kirk McDonald [f], Cullen Newsom [c], Zhe Ning [a,b], Viktor Pěč [g], Sen Qian [a], Vit Vorobel [g], Yifang Wang [a], Jilei Xu [a,b], Changgen Yang [a], Jiawen Zhang [a,*], Qingmin Zhang [a]

[a] Institute of High Energy Physics, CAS, Beijing 100049, China
[b] Graduate University of the Chinese Academy of Sciences, Beijing 100049, China
[c] Department of Physics, University of Houston, Houston, TX 77204-5005, USA
[d] Brookhaven National Laboratory, Upton, NY 11973, USA
[e] Joseph Henry Laboratories, Princeton University, Princeton, NJ 08544, USA
[f] Department of Physics, Princeton University, Princeton, NJ 08544, USA
[g] Charles University, Faculty of Mathematics and Physics, Prague, Czech Republic

ARTICLE INFO

Article history:
Received 9 February 2011
Received in revised form
16 March 2011
Accepted 30 March 2011
Available online 25 May 2011

Keywords:
RPC
Mass production
Quality control/assurance
Cosmic-ray test
Daya Bay

ABSTRACT

Resistive plate chambers will be used in the Daya Bay reactor neutrino experiment to help veto backgrounds created by cosmic-ray muons. The mass production of RPCs began in 2008 and by the end of 2009, 1600 RPCs (3500 m^2) had been produced and tested. This paper describes the production and quality control procedures, and quality assurance using cosmic-ray testing.

1. Introduction

The Daya Bay reactor neutrino experiment [1] is designed to determine the last unknown neutrino mixing angle, θ_{13}, with a sensitivity of $\sin^2 2\theta_{13} < 0.01$ at a 90% confidence level. The main backgrounds at Daya Bay are caused by cosmic-ray muons, which are suppressed by locating the detectors underground. Though this background at Daya Bay is less than 1% of the antineutrino signal [1], efficient muon rejection is vital for a high sensitivity measurement. To accomplish this, the neutrino detectors are submerged in water pools where they are shielded from muon-induced neutrons and gammas by at least 2.5 m of water. Muons will be tracked through the water pools, which are outfitted with PMTs to detect Cherenkov light, and through arrays of resistive plate chambers (RPCs) above the pools.

RPCs are gaseous particle detectors first developed by Santonico et al. [2], in the early 1980s. Due to their simple structure and low cost, they are well-suited for use over large areas. Therefore, RPCs have been an important component in many particle physics experiments such as BaBar [3], BELLE [4], OPERA [5], and those at the LHC [6–8]. A new type of bakelite RPC, which does not use the commonly-applied linseed oil, was developed by the Institute of High Energy Physics (IHEP) in Beijing, and is being used in BESIII [9]. Its performance has been shown to be more than satisfactory for the BESIII muon subsystem [10,11]. The Daya Bay experiment has also chosen to use these RPCs and operate them in streamer mode to detect muons.

The mass production of Daya Bay RPCs began in 2008, and a total of 1600 RPCs (3500 m^2) were finished in 2009. The testing of individual RPCs using cosmic muons was finished at IHEP in 2009. This paper describes the processes of RPC production and quality control, and quality assurance using cosmic ray testing.

2. RPC structure

The Daya Bay experiment will use 1560 RPCs (3330 m^2). All RPCs will be assembled into $2.20 \times 2.17 \times 0.08$ m^3 aluminum boxes as detector modules. A module contains 4 layers of RPCs, each of which consists of one smaller and one larger RPC (1×2.10 m^2 and 1.10×2.10 m^2). The dead-space between each

* Corresponding author.
E-mail address: zhangjw@ihep.ac.cn (J. Zhang).
[1] Now at Institute of Fluid Physics, CAEP.

0168-9002/$ - see front matter © 2011 Elsevier B.V. All rights reserved.
doi:10.1016/j.nima.2011.03.060

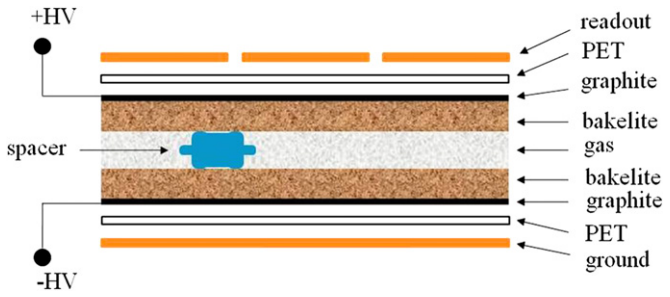

Fig. 1. Basic structure and configuration of an RPC.

larger and smaller RPC is staggered between layers so that the dead-spaces are not vertically aligned. There will be 189 modules, each weighing about 210 kg, divided among three detector sites: 54 at both of the near sites and 81 at the far site.

The basic structure and configuration of a Daya Bay RPC is shown in Fig. 1. Two bakelite plates of thickness 2 mm sandwich a single gas gap of 2 mm. The gas gap size is maintained by polycarbonate button spacers, glued in a $10 \times 10\ \mathrm{cm}^2$ grid. These spacers have a disk-shaped mid-section of 12 mm diameter to increase the surface current path-length (see Fig. 1). Including the mid-section width, the button spacers occupy not more than 1% of the total area of an RPC. Excluding the mid-section, a more accurate estimate of effective dead-area is less than 0.5%. A graphite layer is sprayed on the outer surface of each bakelite plate for the application of high voltage. A 100 μm polyethylene terephthalate (PET) film covers the graphite layer to protect the surface and insulate the readout strips and ground plane from the graphite layer. The readout strips and ground plane are made from sheets of copper-clad FR-4. Signals are picked up on positive side.

3. RPC mass production and quality control

The mass production and quality control of the RPCs consists of bakelite plate production and bulk resistivity measurements, bakelite plate preparation and graphite surface resistivity measurements, RPC assembly and leak testing, and RPC training. After assembly, RPCs are sent to IHEP for training and quality assurance using cosmic-ray testing. The characteristics and performance of all bakelite plates, RPCs and RPC modules are recorded, and have been used to accept or reject RPCs. These data are archived in a MYSQL [12] database accessible through the internet. A unique identification number is associated with each RPC, which will allow tracking long-term behavior.

3.1. Bakelite plate production and bulk resistivity measurements

The bakelite plates are produced at the Li Shen Wood Product Inc. factory in Xinji City. The thickness of the plates is controlled to 2.00 ± 0.02 mm, and the length (width) is about 230 cm (120 cm). The basic material components of the bakelite plates are paper with phenolic and melaminic two-step resins. The proportions of phenol and melamine are controlled to select the bulk resistivity of the bakelite. The paper laminates are heated and compressed between stainless steel plates after being coated with the resin solution. The smoothness of the bakelite plate surfaces is ensured by the outer laminates, which are differently paper coated in a differently-proportioned resin. In addition, new stainless steel press plates were purchased and used for Daya Bay bakelite production to maximize surface smoothness.

After production, bakelite plates are sent to IHEP for measurement of their bulk resistivity. For each plate, the bulk resistivity is measured at nine uniformly spaced regions. A region is covered by two electrodes of 5 cm diameter to which a voltage difference of 4 kV is applied. The current is recorded (as well as temperature and humidity) and used to determine the resistivity. Since the measurements are done in a room that is not temperature-controlled, they are corrected to 20 °C according to the following formula:

$$\rho_{20} = \rho_T 10^{0.06(T-20)} \quad (1)$$

where T is the recorded room temperature in degree Celsius, ρ_T is the average bulk resistivity measured at temperature T, and 0.06 is an empirical parameter taken from a dedicated study performed at IHEP. A bakelite plate is accepted only if the resistivity of each measured region is in the range of $0.5\text{–}2.5 \times 10^{12}\ \Omega\,\mathrm{cm}$ at 20 °C. Fig. 2(a) shows the distribution of the temperature-corrected average bulk resistivity for all measured bakelite plates. Out of 3625 measured plates, 358 (9.9%) were rejected. Fig. 2(b) shows the distribution of the RMS deviation of the 9 measured regions. The average deviation is 6.7% of the average bulk resistivity and 4.4% of the range of acceptance.

Generally, higher resistivity yields lower current and noise rate, but it also implies a longer charge recovery time, which can reduce efficiency, particularly at higher rates. Since the rate at Daya Bay is low, it is sensible to use a higher resistivity, but not so high as to significantly reduce the efficiency. The ranges of bulk and surface (see Section 3.2) resistivities are essentially inherited from RPC development done for BESIII [13].

3.2. Bakelite plate preparation and surface resistivity measurements

The bakelite plates that satisfy the bulk resistivity requirement are sent to Gaonengkedi Ltd. Co. (GNKD) in Beijing, for the assembly of RPCs. Before assembly, all bakelite plates are cut to the dimensions of $1 \times 2.10\ \mathrm{m}^2$ ($1.10 \times 2.10\ \mathrm{m}^2$) for smaller (bigger) RPCs. The size of a bakelite plate is ensured by the positioning pin of the cutting machine, which can make an error less than 0.1%.

After cutting and careful cleaning with ethanol, a layer of special graphite paint is uniformly coated on one side of each bakelite plate using an airbrush, leaving a 1 cm uncoated perimeter. The surface resistivity of the graphite coating is measured about 1 day after painting. The graphite surface resistivity is taken as the mean value of two measured regions. Both of the measured values are required to be in the range of 400–1000 kΩ/□.

After the graphite resistivity measurements, a $1 \times 10\ \mathrm{cm}^2$ strip of copper tape is applied to the graphite near one of its corners for the high voltage connection. Then, a 100 μm PET film coated with a hot-melt glue is applied to the graphite side of the bakelite plate using a laminator.

3.3. RPC assembly and leak testing

RPCs are assembled in a temperature-controlled clean room at GNKD. At the beginning of the assembly, one bakelite plate is put on a platform and cleaned with ethanol. Segments of edge spacers made of ABS, each with a width of 10 mm and thickness of 2 mm, are glued along the perimeter of the bakelite plate. Two gas feed-throughs made of ABS are embedded at both of the shorter sides of the plate, diagonally across from each other. Polycarbonate button spacers, with a mid-section diameter of 12 mm and thickness of 2 mm, are glued onto the plate every $10 \times 10\ \mathrm{cm}^2$. Then, a second bakelite plate is glued to the tops of the edge spacers and button spacers. Finally, the RPC perimeter and regions around the gas feed-throughs are glued externally. For the first 2 h after gluing, the RPC is vacuumed to about 8% atmospheric pressure by a vacuum pump, after which it is sealed. This process is to prevent the gas gap from expanding beyond the height of the spacers.

After 2 days of curing, the gas-tightness of the RPC is tested by applying an over-pressure of 300 mm of water (30 mbar) to the

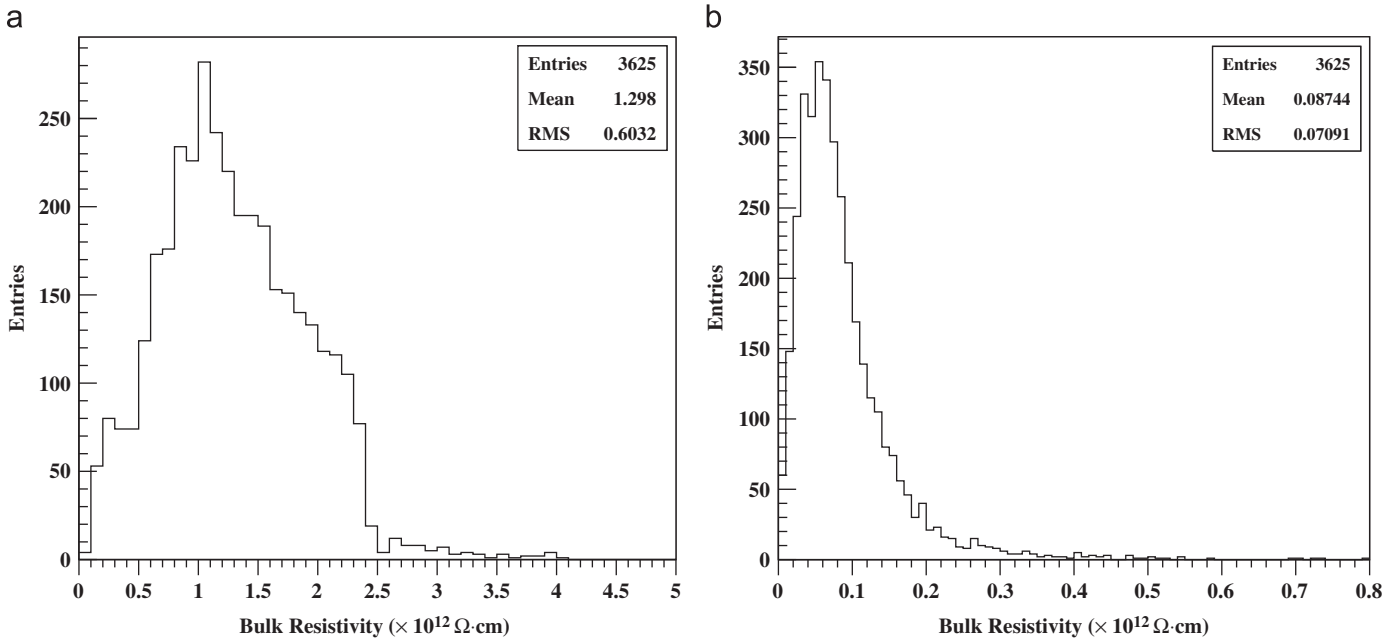

Fig. 2. Distributions of bakelite average bulk resistivity (a) and RMS deviation of the 9 measured regions (b).

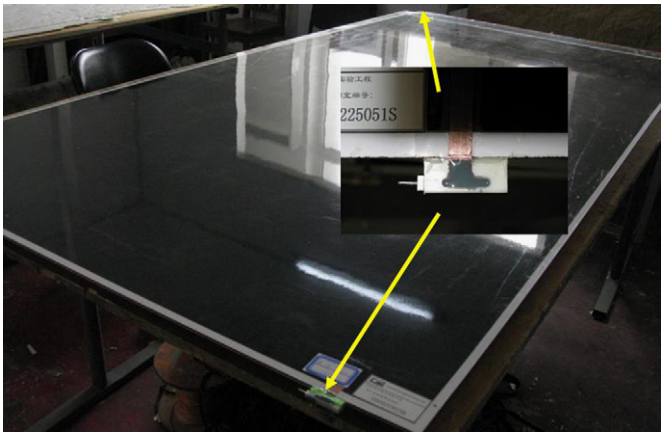

Fig. 3. Fully assembled Daya Bay RPC. The inset shows the epoxy-covered HV connection within a gas feed-through connector and the copper tape extending onto the graphite electrode.

gas gap for 30 min. RPCs are accepted only if the decrement in the height of the water level is less than 2 mm (assuming a 25 cm^3/min flow rate, which is expected at Daya Bay, this decrement would correspond to 0.1% leakage). Failed RPCs are re-glued along their perimeters and re-tested.

Finally, two small copper tubes with HV connection pins are each carefully soldered within the gas feed-through connectors to one of the strips of copper tape on either graphite electrode. The remaining exposed copper tape and soldered areas are covered by an insulating epoxy. Fig. 3 shows a picture of a fully assembled RPC at IHEP and a gas feed-through and HV connector.

3.4. RPC training

Generally, newly-made RPCs have noise rates, which are high enough to decrease their efficiency. So, before cosmic-ray testing, a "training" process is performed. Up to 10 kV is applied to an RPC for at least about 48 h while flowing only argon at 100 cm^3/min. Since there is no quenching gas component, the current becomes extremely high: about two to three orders of magnitude higher than normal operating current. Due to the limit of the high voltage (HV) modules, the current through an RPC is kept below 1 mA by adjusting the HV. Fig. 4(a) shows the currents through 7 typical RPCs during training. After an initial increase, which we believe to be at least partly due to self-heating, the currents decrease and usually become relatively stable after 50 h. Fig. 4(b) shows the distribution of training time of all RPCs, where each entry represents 8 RPCs that were trained simultaneously. After training, the current through a newly-made RPC at normal operating conditions will have reduced by an order of magnitude.

Training also provides an opportunity to cross-check the resistivity of the bakelite plates. From the slopes of current versus voltage plots, we found resistivities to be slightly larger ($\sim$20% average percentage error) than those from the electrode measurements. We attribute most of this discrepancy to the higher temperature of the self-heated bakelite, which is not measured. Finally, we note that while training, the conductive quality of the RPC HV connections is also under test.

4. Quality assurance (cosmic ray testing)

Cosmic-ray testing is the last step in quality assurance before putting RPCs into modules. The efficiency, singles counting rate (SCR), and dark current of the RPCs are measured. The criteria of acceptance are that the efficiency should be higher than 94%, SCR lower than 0.80 Hz/cm^2, and dark current lower than 10 $\mu A/m^2$, at 8.0 kV and a 50 mV signal threshold. The efficiency criterion is motivated by the requirement that the total muon detection efficiency of the Daya Bay muon veto system (the RPCs and the water Cherenkov pools) reaches 99.5%. The SCR and current criteria have no specific demands; hence, they are simply chosen to reject the most extreme RPCs, which are the RPCs most likely to become problematic after a long time running.

4.1. Testing system and procedure

The RPCs are tested in a dedicated testing room with the temperature controlled to $20\pm2\,^{\circ}C$ and the relative humidity controlled to $33\%\pm10\%$. The atmospheric pressure has varied from

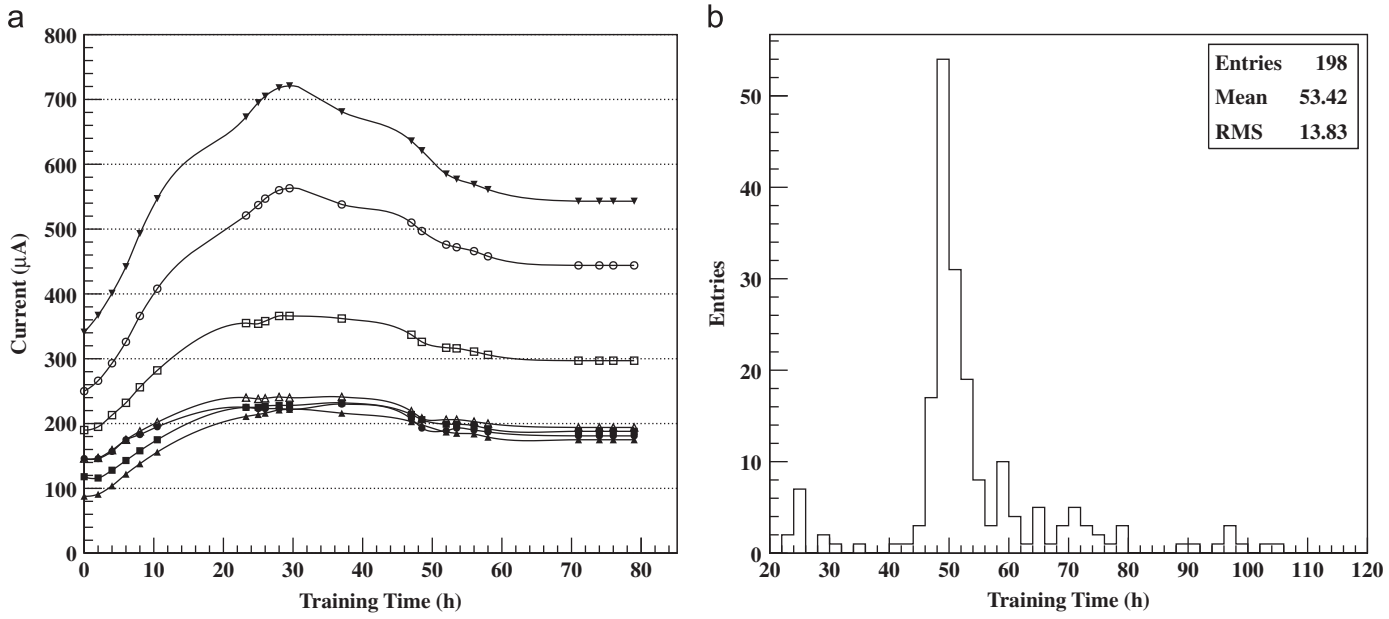

Fig. 4. Training currents of 7 RPCs versus time (a) and the training time distribution of RPCs (each entry represents 8 RPCs) (b).

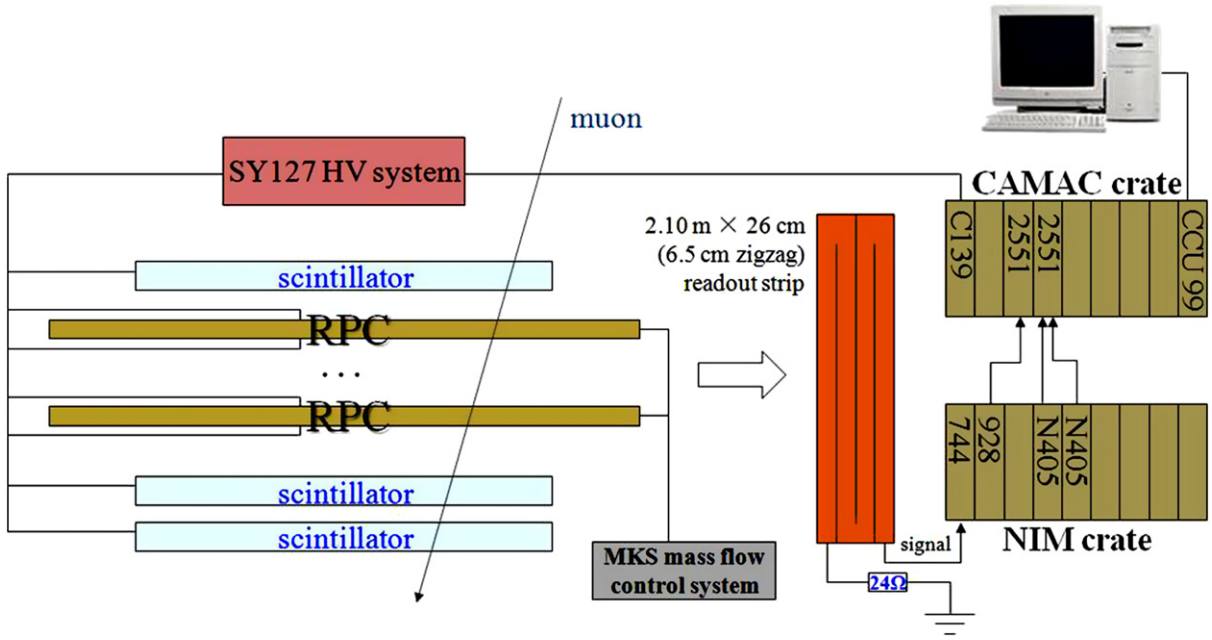

Fig. 5. Diagram of the RPC cosmic-ray testing system.

995 to 1035 mbar over the entire testing period with an average of 1015 mbar. The RPCs are brought into the room at least 5 h before testing to reach thermal equilibrium. They are tested in streamer mode with the gas mixture argon:R134a:isobutane=53:43:4. For performance of Daya Bay RPCs with the baseline (argon:R134a: isobutane:SF_6=65.5:30:4:0.5) and other gas mixtures, see Ref. [14]. The fractions of the gas components are ensured by an MKS mass-flow control system to a measured accuracy of 1%. The total gas flow rate is set at 200 cm^3/min. Before testing, 6 RPCs are connected in series by gas tubes and flushed with at least 6 or 7 volumes of gas. This is sufficient since the RPCs are initially filled with argon from training. Three plastic scintillators, each with the dimensions of 1×1 m^2, are used as a telescope for triggering on muons. A muon trigger requires a three-fold coincidence of the signals from the three scintillators. The trigger rate is about 20 Hz. A diagram of the testing system is shown in Fig. 5.

As will be the case at Daya Bay, RPC signals are read out from copper-clad FR-4 zigzag strips, as shown in Fig. 6(a). Each readout strip zigzags across 26 cm $\times$ 2.10 m in three turns: one turn at one of the 26 cm sides and two turns at the opposite side. This gives a signal quality equivalent to that of a readout strip with dimensions of 6.5 cm $\times$ 8.4 m. It provides taller and narrower pulses without requiring more readout channels. Each RPC uses four readout strips, each terminated at 24 Ω, and four readout channels, which are discriminated at a pulse height threshold of 50 mV. Fig. 6(b) shows some typical signals ($\approx$ 100 mV) read out by an oscilloscope.

For every RPC, signals from the four readout strips are discriminated and then "Logical-OR"ed together as RPC signal to determine the SCR. This RPC signal is then "Logical-AND"ed with the 3-fold coincidence trigger of the scintillators as 4-fold coincidence. The resulting number of 4-fold coincidences is divided by the number of 3-fold scintillator triggers to determine the efficiency of an RPC.

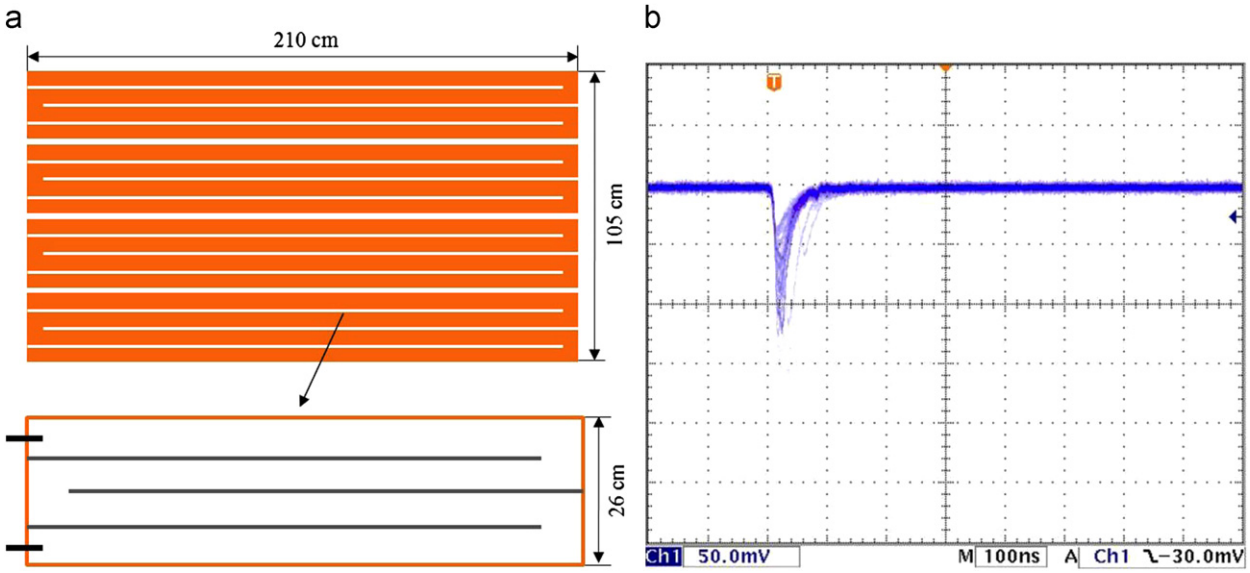

Fig. 6. Zigzag readout strips and the connection points on a single strip (a), and typical signals from an RPC on an oscilloscope (b).

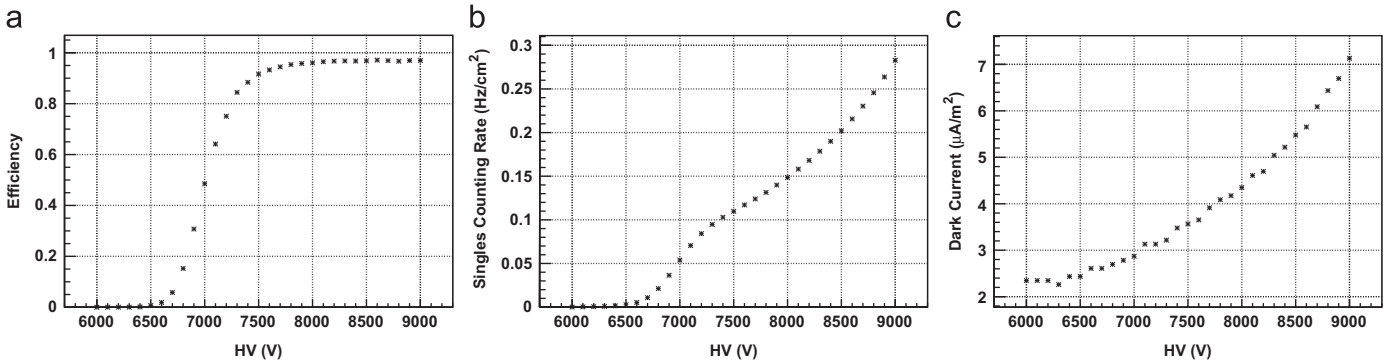

Fig. 7. Efficiency (a), singles counting rate (b), and dark current (c) versus high voltage for one RPC.

High voltage (HV) is supplied to the RPCs by a CAEN SY127 system with a precision of 1 μA on each current channel. A CAMAC C139 module adjusts the HV as commanded by custom DAQ software based on ROOT [15]. The data of 3-fold coincidences, 4-fold coincidences, singles counts, and currents are recorded by the custom software. The temperature, pressure, and humidity of the room are also recorded during each test.

For the testing, the HV is raised from 6.0 to 9.0 kV in steps of 0.1 kV for at least 5 cycles. Efficiencies and singles counts are measured for 100 s at each HV. Thus, each test counts about 5 cycles × 100 s × 20 Hz = 10,000 4-fold coincidences for each RPC at each plateau voltage.

4.2. Testing results

With the gas mixture argon:R134a:isobutane = 53:43:4 and pulse height threshold 50 mV, the RPCs usually become 94% efficient around 7.4–7.7 kV, and reach peak efficiency (about 97%) around 8.6–8.9 kV. The SCR and dark current begin to increase quickly around 8.2–8.4 kV.

The evaluation voltage of the RPCs was chosen to provide high efficiency without excessive current and SCR. Based on the aforementioned observations, this voltage should be chosen between 7.7 and 8.2 kV. Since the voltage across the gas gap is directly proportional to the gas density, which depends on temperature (T) and pressure (P) [16], the evaluation voltage of all RPCs was selected to be in the middle of this range (8.0 kV) at the standard conditions, $T_0 = 293$ K and $P_0 = 1010$ mbar. Fig. 7 shows the efficiency (a), SCR (b), and dark current (c) versus HV for a typical RPC at the standard conditions.

4.2.1. Efficiency

An RPC is expected to have an efficiency no lower than 94% and a plateau longer than 1 kV. Fig. 8 shows the efficiency distribution of all measured RPCs at 8 kV. The average efficiency is 95.34%. About 11% (171 RPCs) have efficiencies below 94%, which is below the acceptance criterion. The average efficiency of all accepted RPCs is 96.05%.

Fig. 8 also shows the efficiency distribution of all measured RPCs at 8.7 kV, which is around the voltage at which the RPCs reach their highest efficiency. The average efficiency of all RPCs at 8.7 kV is 96.13%, which is a 0.79% increase from 8.0 kV. Additionally, some of the lower-efficiency RPCs in the left tail of the distribution at 8.0 kV move closer to the primary peak of the distribution at 8.7 kV, which decreases the RMS deviation by 0.31% (a 13% percentage difference). The gas gap sizes of these "late" RPCs are presumed to be above average.

To produce an identical electric field across a larger gas gap, a larger voltage needs to be applied. Fig. 9(a) shows the distributions of the voltage at which RPCs reach 50% efficiency for both accepted and rejected RPCs. The efficiency curve is linear in this

region, which indicates that the electric field is the dominant factor determining the efficiency. Thus, around 50% efficiency, a change in voltage simply corresponds to a change in gap size. With a RMS deviation of 132 V about a mean of 6861 V for accepted RPCs, the deviation of the gap is estimated to be 2 mm × 132 V/6861 V = 38 μm, or 1.9%, which is about twice the expected mechanical tolerance of the button spacers. The voltage distributions in Fig. 9 have been corrected for climate variations and the voltage dropped across the bakelite plates; thus, they can be attributed to geometric and mechanical effects.

A similar distribution can give the deviation in voltage near the operating efficiency, which is useful when considering operating voltage. Fig. 9(b) shows the distribution of the knee voltage for accepted and rejected RPCs. The knee voltage is defined at the intersection of two lines on the efficiency curve: a horizontal line at the average plateau efficiency and a line fit to the three points that are closest to 50% efficiency. At this voltage (7112 V mean), the RMS deviation of accepted RPCs is 141 V, which is similar to the deviation at 50% efficiency. This shows that the voltage at which RPCs approach their individual operating efficiencies is primarily determined by the gap size. Additionally, the means and RMS deviations of rejected RPCs are 6978 and 7250 V, and 218 and 238 V, for the 50% efficiency and knee voltages, respectively. The higher means are indicative of larger gaps among rejected RPCs. From Fig. 9(b), it is seen that 0.4–0.5 kV must be added to the mean of the knee voltage distribution to allow the majority of RPCs to reach their individual operating efficiencies.

4.2.2. Singles counting rate (SCR)

The SCR at 8 kV is required to be lower than 0.80 Hz/cm^2 with a 50 mV threshold. Fig. 10 shows the SCR distributions of all accepted and rejected RPCs at 8 kV with a 50 mV threshold, just after training. The average SCR of accepted RPCs is 0.150 Hz/cm^2. 19 RPCs (1.2%) failed the SCR criterion, of which 6 also failed the efficiency criterion. The average SCR of all RPCs is 0.152 Hz/cm^2.

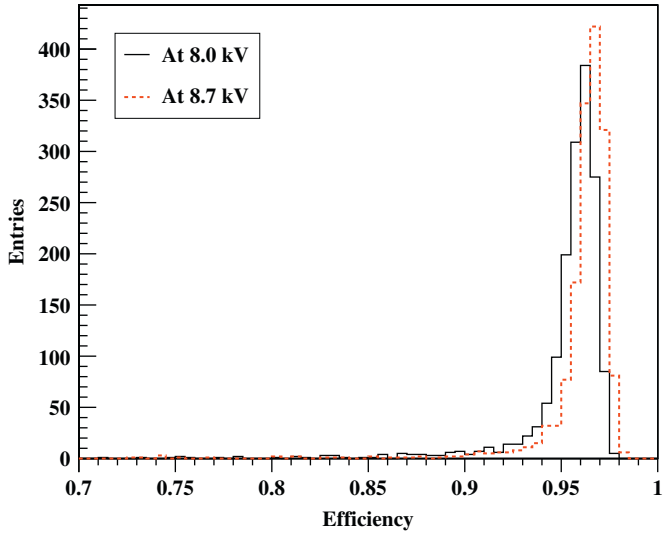

Fig. 8. Efficiency distributions of all measured RPCs at 8 kV (a) and 8.7 kV (b) with a 50 mV threshold.

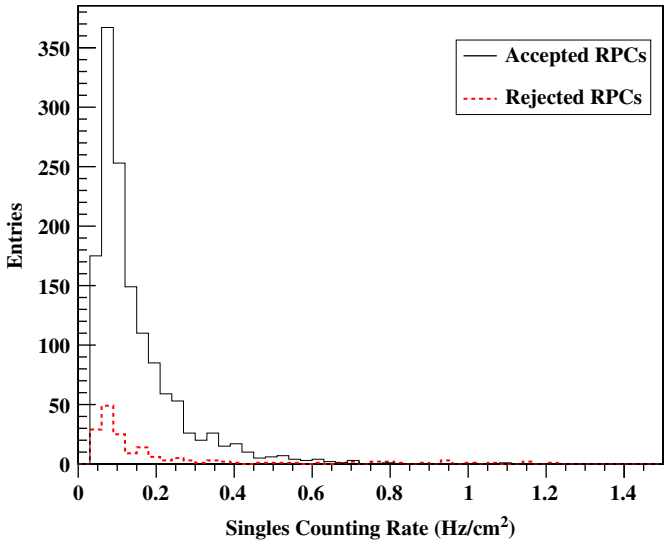

Fig. 10. SCR distributions of all accepted and rejected RPCs at 8 kV with a 50 mV threshold.

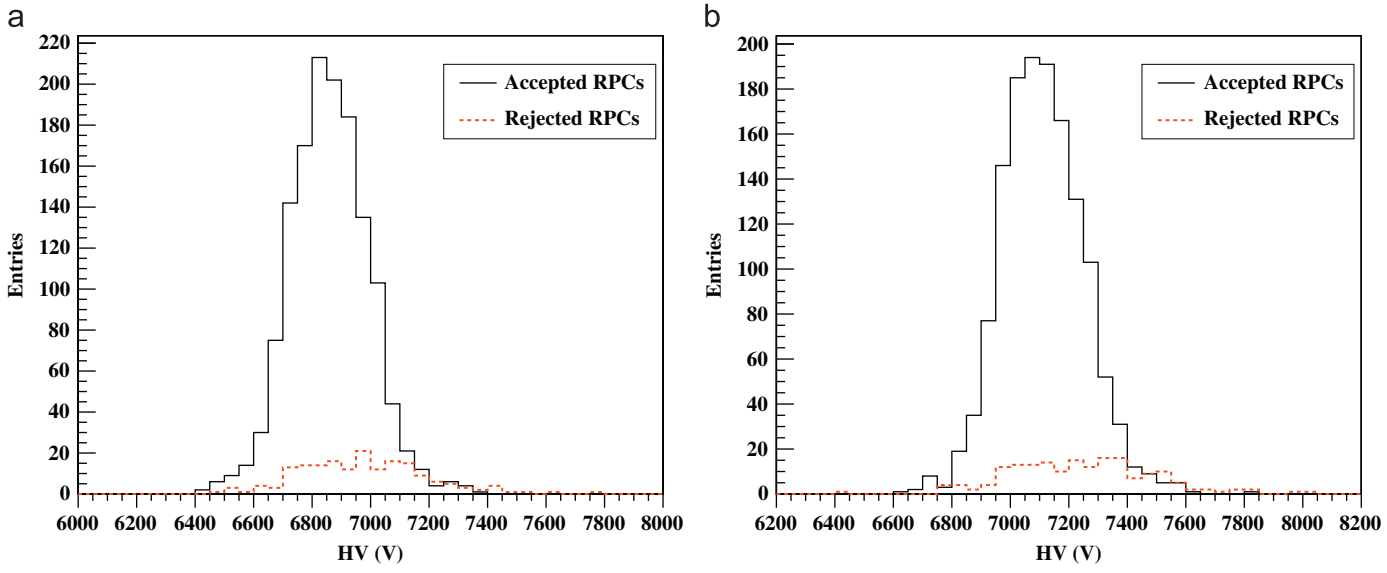

Fig. 9. Voltage distributions of all accepted and rejected RPCs at 50% efficiency (a) and the knee (b).

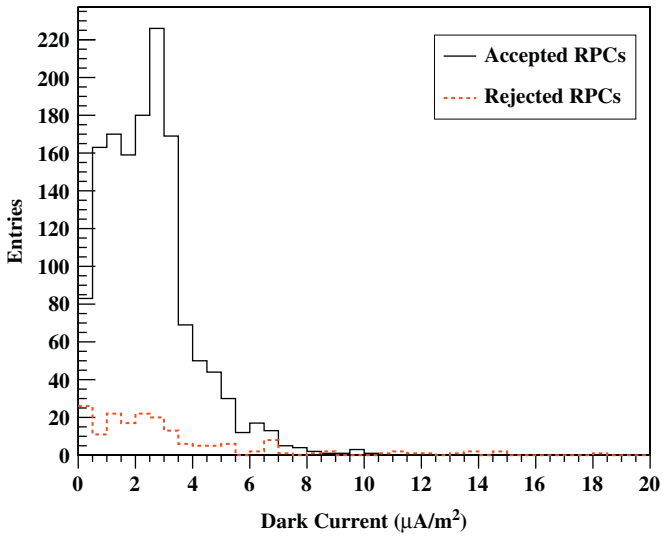

Fig. 11. Dark current distributions of all accepted and rejected RPCs at 8 kV.

4.2.3. Dark current

The dark current at 8 kV is required to be lower than 10 μA/m^2. Fig. 11 shows the dark current distributions of all accepted and rejected RPCs at 8 kV. The average dark current of accepted RPCs is 2.54 μA/m^2. Only 13 RPCs (0.8%) failed the current criterion, of which 12 also failed the efficiency or high SCR criteria. The average dark current of all RPCs is 2.55 μA/m^2.

5. Discussion

The fraction of RPCs that failed to meet the efficiency criterion (11%) is much larger than those of the SCR or current criteria (1%). This is simply because the SCR and current criteria are less stringent. However, RPCs that simultaneously fail the SCR and efficiency criteria may indicate a correlation. We also observe that the average maximum efficiency of accepted RPCs is 96.6% while the loss due to the dead-areas created by the button spacers is about 0.5%; hence, 3% inefficiency is not considered. We are currently investigating these issues and hope to publish the findings in the future.

In our experience, it is found that some RPCs that have low efficiency can be improved by retraining at a higher temperature. At a higher temperature, the bulk resistivity of the bakelite decreases (see Eq. (1)), enabling higher currents at the same HV; thus, augmenting the effects of training. After retraining, the noise rate and current are further decreased, and so the efficiency is improved. Even after training, it is common for the SCR (and dark current) to continue decreasing over weeks of normal operation [17,10].

6. Conclusion

The production and quality control and assurance of about 1600 RPCs has been completed for the Daya Bay reactor neutrino experiment. The rejection rate after assembly is about 12%. Most (11%) of these RPCs are rejected due to an efficiency slightly below the acceptance criterion (94% efficiency). Of those that pass the efficiency criterion, few (1%) are rejected due to a high SCR or high dark current (0.80 Hz/cm^2 and 10 μA/m^2). A second batch of RPCs is being produced to replace the rejected RPCs. RPCs that satisfy the selection criteria are assembled into RPC modules, which are also being tested. Details of module testing will be presented in another publication.

Acknowledgments

IHEP at the Chinese Academy of Sciences is supported by the China National Science Foundation and the Ministry of Science and Technology of the People's Republic of China. The University of Houston, Brookhaven National Laboratory, and Princeton University are supported by the United States Department of Energy. Charles University is supported by projects MSM0021620859 and ME08076 of the Ministry of Education, Youth and Sports of the Czech Republic, and 202/08/0760 of the Czech Science Foundation. We thank the Gaonengkedi Science and Technology Company and Weiping Niu for their work on RPC construction.

References

[1] Daya Bay Collaboration, arXiv: hep-ex/0701029, 2007.
[2] R. Santonico, et al., Nucl. Instr. and Meth. A 187 (1981) 377.
[3] BaBar Collaboration, Nucl. Instr. and Meth. A 479 (2002) 1.
[4] BELLE Collaboration, Nucl. Instr. and Meth. A 479 (2002) 117.
[5] M. Guler et al., CERN/SPSC 2000-028, SPSC/P318, LNGS P25/2000, July 10 2000;
M. Guler et al., CERN/SPSC 2001-025, SPSC/M668, LNGS-EXP 30/2001 Add.1/01, August 21 2001.
[6] ALICE Collaboration, CERN/LHCC 99-22, 13 August 1999.
[7] ATLAS Muon Collaboration, CERN/LHCC 97-22, 5 June 1997.
[8] CMS Collaboration, CERN/LHCC 97-32, 15 December 1997.
[9] The BESIII Detector, IHEP-BEPCII-SB-13, IHEP, Beijing.
[10] J. Han, et al., Nucl. Instr. and Meth. A 577 (2007) 552.
[11] Y. Xie, et al., Nucl. Instr. and Meth. A 599 (2009) 20.
[12] 〈http://www.mysql.com/〉.
[13] Y. Xie, et al., Chin. Phys. C (HEP & NP) 31 (1) (2007).
[14] L. Ma, et al., Chin. Phys. C (HEP & NP) 34 (8) (2010) 1116.
[15] 〈http://root.cern.ch〉.
[16] M. Abbrescia, et al., Nucl. Instr. and Meth. A 359 (1995) 603.
[17] J. Zhang, et al., Nucl. Instr. and Meth. A 540 (2005) 102.